Klymkowsky, M., & Stroud, R. (1979) *J. Mol. Biol. 128*, 319.
Laemmli, U. (1970) *Nature (London) 227*, 680.
Lennon, V. A., Lindstrom, J. M., & Seybold, M. E. (1975) *J. Exp. Med. 141*, 1365.
Lindstrom, J. (1979) *Adv. Immunol.* (in press).
Lindstrom, J., & Patrick, J. (1974) in *Synaptic Transmission and Neuronal Interaction* (Bennett, M. V. L., Ed.) pp 191–216, Raven Press, New York.
Lindstrom, J., & Einarson, B. (1979) *Muscle Nerve 2*, 173.
Lindstrom, J. M., Einarson, B., Lennon, V. A., & Seybold, M. E. (1976a) *J. Exp. Med. 144*, 726.
Lindstrom, J. M., Engel, A. G., Seybold, M. E., Lennon, V. A., & Lambert, E. H. (1976b) *J. Exp. Med. 144*, 739.
Lindstrom, J., Lennon, V., Seybold, M., & Whittingham, S. (1976c) *Ann. N.Y. Acad. Sci. 274*, 254.
Lindstrom, J. M., Seybold, M. E., Lennon, V. A., Whittingham, S., & Duane, D. D. (1976d) *Neurology 26*, 1054.
Lindstrom, J., Campbell, M., & Nave, B. (1978a) *Muscle Nerve 1*, 140.
Lindstrom, J., Einarson, B., & Merlie, J. (1978b) *Proc. Natl. Acad. Sci. U.S.A. 75*, 769.
Lindstrom, J., Merlie, J., & Yogeeswaran, G. (1979) *Biochemistry* (preceding paper in this issue).
Merlie, J. P., Changeux, J.-P., & Gros, F. (1977) *J. Biol. Chem. 253*, 2882.
Merlie, J., Heinemann, S., Einarson, B., & Lindstrom, J. (1979) *J. Biol. Chem. 254*, 6328.
Moore, H., Hartig, P., Wilson, C., & Raftery, M. (1979) *Biochem. Biophys. Res. Commun. 88*, 735.
Nathanson, N., & Hall, Z. (1979) *Biochemistry 18*, 3392.
Newsome-Davis, J., Pinching, A. G., Vincent, A., & Wilson, S. (1978) *Neurology 28*, 266.
Patrick, J., & Lindstrom, J. (1973) *Science 180*, 871.
Patrick, J., Lindstrom, J., Culp, B., & McMillan, J. (1973) *Proc. Natl. Acad. Sci. U.S.A. 70*, 3334.
Raftery, M. A., Vandlen, R. L., Reed, K. L., & Lee, T. (1975) *Cold Spring Harbor Symp. Quant. Biol. 40*, 193–202.
Reynolds, J. A., & Karlin, A. (1978) *Biochemistry 17*, 2035.
Shorr, R. G., Dolly, O., & Bernard, E. (1978) *Nature (London) 274*, 283.
Sobel, A., & Changeux, J.-P. (1977) *Biochem. Soc. Trans. 5*, 511.
Sobel, A., Heidmann, T., Hofler, J., & Changeux, J.-P. (1978) *Proc. Natl. Acad. Sci. U.S.A. 75*, 510.
Tarrab-Hazdai, R., Geiger, B., Fuchs, S., & Amsterdam, A. (1978) *Proc. Natl. Acad. Sci. U.S.A. 75*, 2497.
Vandlen, R., Wilson, C., Eisenach, J., & Raftery, M. (1979) *Biochemistry 18*, 1145.
Weill, C., McNamee, M. G., & Karlin, A. (1974) *Biochem. Biophys. Res. Commun. 61*, 997.
Weinberg, C., & Hall, Z. (1979) *Proc. Natl. Acad. Sci. U.S.A. 76*, 504.

Spin-Label Studies of Lipid Immobilization in Dimyristoylphosphatidylcholine-Substituted Cytochrome Oxidase†

Peter F. Knowles, Anthony Watts, and Derek Marsh*

ABSTRACT: Yeast cytochrome oxidase complexes have been prepared in which ≥99% of the endogenous lipid has been substituted by dimyristoylphosphatidylcholine and the lipid chain immobilization has been studied by spin-label spectroscopy. The ESR spectra of a C(14) phosphatidylcholine spin-label consist of both an immobilized and a fluid lipid bilayer component for all complexes, the proportion of the former increasing with increasing protein/lipid ratio. Computer difference spectroscopy has been used to obtain the two different spectral components and to determine their relative proportions. Lipid/protein titration of the complexes, in the region where the proportion of fluid lipid exceeds that of the immobilized, reveals that a constant number of lipid molecules (55 ± 5) per protein are immobilized. This is attributed to a first or boundary shell of lipids associated with the protein, which is then surrounded by fluid bilayer. Estimates of motional correlation times from the immobilized lipid difference spectrum give values of ≥50 ns, suggesting that the rate of exchange between bilayer and boundary lipids is probably at least 1 order of magnitude slower than the rate of lateral diffusion of unperturbed bilayer lipids. The variation of the spectral splittings and line widths of the fluid-component difference spectra with lipid/protein ratio shows that a second shell of lipids is perturbed by the protein, a third shell is less strongly perturbed, and a further two to three shells may be still weakly perturbed. Thus, the immobilization of the lipid may extend out to approximately six shells from the protein. These structural properties correlate with measurements of the enzyme activity which show a rapid decrease in activity with decreasing lipid/protein ratio for complexes containing less than the minimum immobilized "boundary" layer of lipid and a smaller but steady increase in activity with increasing lipid/protein ratio for complexes with from one to six shells of lipid.

Lipid–protein interactions are potentially important determinants of membrane structure and function, not only from the point of view of regulation of membrane-bound enzymes and transport proteins but also with regard to the incorporation of proteins into the lipid matrix, hence maintaining the structural integrity of the membrane envelope. Thus, it is of considerable interest to investigate the interaction between integral membrane proteins and the shells of lipid immediately surrounding the protein. It is these lipid molecules which are most likely to affect the protein conformation, to be responsible for sealing the protein into the bilayer, and to form the means of communication with the bulk bilayer phase.

Specific immobilization of a boundary layer of lipid surrounding the integral membrane protein cytochrome oxidase

† From the Max-Planck-Institut für biophysikalische Chemie, Abt. Spektroskopie, D-3400 Göttingen, Federal Republic of Germany (A.W. and D.M.), and the Astbury Department of Biophysics, Leeds University, Leeds LS2 9JT, England (P.F.K.). *Received April 20, 1979; revised manuscript received June 29, 1979.*

0006-2960/79/0418-4480$01.00/0

was first demonstrated by Jost et al. (1973a) using ESR[1] spin-label techniques. Warren et al. (1974a) have proposed the requirement of a first lipid shell or annulus to support enzymic activity of the Ca^{2+}–Mg^{2+} ATPase from sarcoplasmic reticulum. Curatolo et al. (1977) have deduced that three to four lipid shells around the protein exhibit perturbed phase-transition characteristics in myelin proteolipid apoprotein–DMPC recombinants. Vaz et al. (1978) have interpreted the kinetics of incorporation of cytochrome b_5 into lipid vesicles as indicating that approximately five shells of lipids are perturbed by the protein. Theoretical treatments also suggest that several lipid shells are perturbed by the protein (Marčelja, 1976; Owicki et al., 1978). On the other hand, NMR experiments with rhodopsin-containing rod outer segment disk membranes (Brown et al., 1977) and with reconstituted Ca^{2+}ATPase (Stoffel et al., 1977) and cytochrome oxidase (Seelig & Seelig, 1978) lipid complexes have led to the suggestion that the lipid shells in immediate contact with the protein exchange with the bilayer lipids at a rate which is rapid on the NMR time scale.

We have investigated certain aspects of the cytochrome oxidase system in more detail using a reconstitution in which the whole of the endogenous lipid has been substituted by a single phospholipid type, dimyristoylphosphatidylcholine (DMPC). Enzyme complexes were prepared at various lipid/protein ratios, and the interaction with the lipid chains was studied by means of the ESR spectra of a phosphatidylcholine spin-label introduced into the complexes together with the substituting lipid. ESR spin-label methods offer a time window which is sufficiently fast that, even if the exchange rate between the various lipid shells is as rapid as in unperturbed lipid bilayers (Scandella et al., 1972; Träuble & Sackmann, 1972), spectra from the individual shells might be resolved, provided that the mobility differences between them are large enough. Thus, spin-label studies can provide one way of looking directly at the properties of the lipid shells immediately adjacent to the protein. In particular, we have studied the stoichiometry of the immobilized boundary lipid component at the higher lipid/protein ratios for which the fluid lipid population is greater than the immobilized one and have examined the perturbation of the lipid shells beyond the first boundary layer. Additionally, we have attempted to assess the degree of immobilization of the boundary layer component as a function of lipid/protein ratio and, hence, to give estimates of the rate of exchange between the boundary layer and subsequent shells.

Experimental Section

Materials. L-α-Dimyristoylphosphatidylcholine (DMPC) was obtained from Fluka (Buchs, Switzerland) and ran as a single spot in thin-layer chromatograms. Gas–liquid chromatography revealed that the lipid was composed of 97.5% C14:0 chains (Watts et al., 1978). Cholic acid, obtained from Sigma Chemical Co. (St. Louis, MO), was recrystallized twice from ethanol–water (2:1 v/v) before conversion to the sodium salt. The phosphatidylcholine spin-label 14-PCSL was prepared according to the methods of Hubbell & McConnell (1971) and Boss et al. (1975). Cytochrome oxidase was isolated from baker's yeast as described by Virji & Knowles (1978) and had comparable homogeneity and enzymic activity

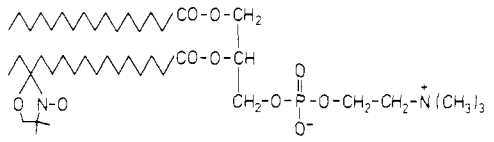

14-PCSL

to that described by Eytan & Schatz (1975). The molecular weight of cytochrome oxidase was taken to be 200000. The buffer used throughout was Tris (10 mM), KCl (1.0 M), and sucrose (1% w/v) adjusted to pH 7.0 at 20 °C (TKS buffer). Cytochrome *c* (Sigma; Grade VI) was reduced with dithionite according to the method of Yonetani & Ray (1965). [*carboxyl*-^{14}C]Cholic acid sodium salt, 59.5 mCi/mol, was obtained from the Radiochemical Centre, Amersham, U.K.

(*1*) *Lipid Exchange and Preparation of Lipid/Protein Complexes.* The endogenous lipid and detergent present in the native cytochrome oxidase was replaced by DMPC by using cholate-mediated exchange (Warren et al., 1974b). The enzyme was incubated at 25 °C for 30 min with a 1000-fold molar excess of DMPC in 0.2% cholate and then precipitated at 0 °C by dropwise addition of saturated ammonium sulfate (pH 7.0) to 35% saturation. Following centrifugation (80000*g* for 10 min), the pellet was resuspended in a second exchange medium, identical with the first, and the whole exchange procedure was repeated for a total of 3 times. Samples with different lipid/protein ratios were prepared by one of two methods. For complexes with lipid/protein ratios less than 100:1, the 3-times-exchanged enzyme was incubated with a 1000-fold molar excess of DMPC (including 2 mol % spin-labeled phospholipid) in the presence of different cholate concentrations (0.2–0.5%) for 30 min at 25 °C and then precipitated by ammonium sulfate addition and centrifuged. The pellets were then resuspended in the stock TKS buffer containing 0.2% sodium cholate to give a final sample volume of 0.5 mL. Complexes extensively depleted of lipid were prepared from samples precipitated from the DMPC medium containing 0.5% cholate as described above by resuspending in TKS buffer containing 0.5% cholate and reprecipitating with ammonium sulfate. After centrifugation the depleted sample was finally resuspended in TKS buffer containing 0.2% sodium cholate. For complexes with lipid/protein ratios greater than 100:1, the 3-times-exchanged enzyme was incubated with appropriate amounts of DMPC (containing 2 mol % added phospholipid spin-label) in the presence of 1.25% cholate for 30 min at 25 °C. The sample was then diluted 10-fold with Tris (10 mM) and KCl (1.0 M), pH 7.0, buffer and centrifuged at 35000 rpm for 30 min (Spinco 40 rotor), and the clear, yellow-green supernatant was concentrated to a volume of 0.5 mL by vacuum dialysis at 0 °C (Sartorius ultrafilter). Cholate was removed from all samples by dialysis, against a 2000-fold volume excess of TKS buffer containing Amberlite XAD-2 (B.D.H., Poole, England), at 15 °C for 15 h. [^{14}C]Cholate assays indicated that under these conditions the residual cholate is reduced to approximately 5 mol/mol of protein. Samples of dialyzed enzyme complexes subjected to sucrose density gradient centrifugation (4–6% sucrose in Tris (10 mM) and KCl (0.1 M) buffer, pH 7.0) for 2 h at 25000 rpm (Spinco SW27 rotor) exhibited a single band whose position in the gradient was dependent on the lipid/protein ratio of the complex.

(*2*) *Analytical Methods.* Enzyme activity was measured spectrophotometrically at 550 nm on a Cary 14 spectrophotometer at room temperature by following the oxidation of ferrocytochrome *c* as described by Smith (1955). The assay mixture consisted of potassium phosphate (40 mM; pH 6.7)

[1] Abbreviations used: DMPC, L-α-dimyristoylphosphatidylcholine; 14-PCSL, β-14-(4′,4′-dimethyloxazolidine-*N*-oxyl)stearoyl-γ-palmitoyl-α-phosphatidylcholine; Tris, 2-amino-2-(hydroxymethyl)-1,3-propanediol; ESR, electron spin resonance; TKS buffer, 10 mM Tris, 1.0 M KCl, and 1% (w/v) sucrose, pH 7.0, buffer.

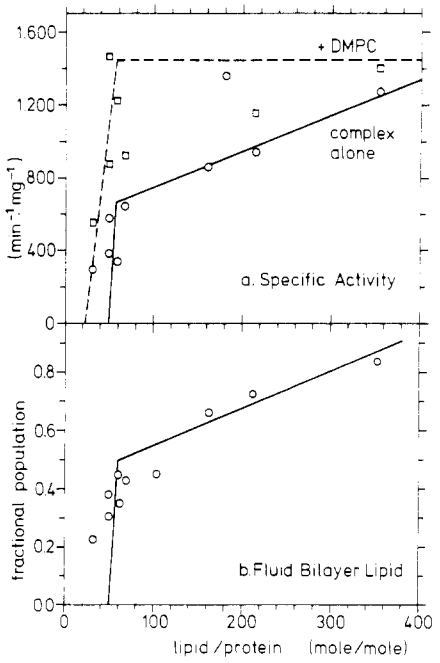

FIGURE 1: (a) Specific activity of cytochrome oxidase–DMPC complexes as a function of lipid/protein ratio, without (–O–) and with (--□--) preincubation with excess DMPC. (b) Fraction of lipid in the complex which is present as the fluid bilayer, as deduced from spin-label spectra.

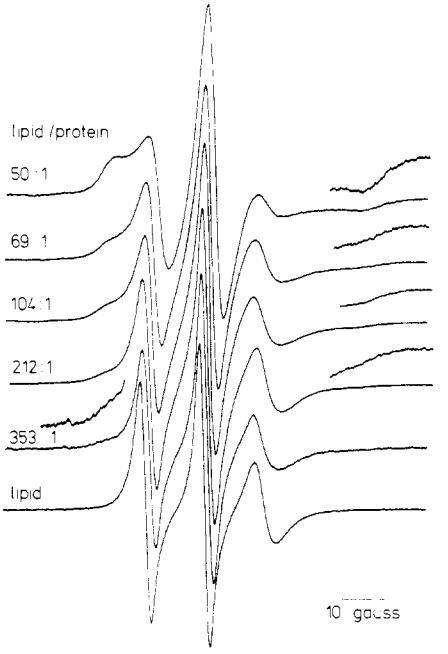

FIGURE 2: ESR spectra of 14-PCSL spin-label in cytochrome oxidase–DMPC complexes of various lipid/protein ratios at 32 °C.

and ferrocytochrome *c* (30 μM) in a final volume of 1.8 mL. Enzyme samples were incubated in TKS buffer containing 0.5% cholate for 60 min at 0 °C before dilution into the assay mixture. The final cholate concentration in this "dilution assay" system was 3.1×10^{-3}%. In some cases DMPC (1000 times molar excess) was added back to the enzyme in the cholate incubation step. Activities are quoted as the specific first-order rate constant [minute^{-1} (milligram of protein)$^{-1}$] under the specified assay conditions and are normalized to a 1.8-mL assay volume. Protein concentration was determined by the method of Dulley & Grieve (1975), and lipid phosphate concentration was determined according to Eibl & Lands (1969).

(*3*) *ESR Spectroscopy.* Samples containing typically 0.5–1 mg of protein were contained in 1-mm (i.d.) capillaries accommodated within standard 4-mm quartz ESR tubes containing silicon oil for thermal stability. ESR spectra were recorded on a Varian E-12 9-GHz spectrometer equipped with a nitrogen gas flow temperature regulation system. Spectra were digitized on paper tape (1000 points/100 G) by using a Hewlett-Packard 3450B/2547A/2753A data collection system and processed on a PDP 11/34 computer with a Tektronix 4006 display. Spectra were scaled to a constant second integral prior to subtraction, and difference spectra were examined at up to 10-fold vertical expansion in order to obtain good end points in the subtractions.

Results

The specific activity of the various DMPC-substituted complexes is given in Figure 1a as a function of the lipid/protein mole ratio. All activities were measured by the dilution assay method since this ensures direct accessibility of the substrate to the enzyme and also allows adding back of lipid to assess the degree of regenerability of the activity. When assayed directly, without these measures to ensure substrate accessibility, the activity was very low for complexes of all lipid/protein ratios. Figure 1a shows that there is an abrupt decrease in enzymatic activity of the complexes at a level of around 50 lipid molecules/protein. For complexes assayed without lipid addition, there is a gradual increase in activity with the lipid/protein ratio at above the critical 50:1 ratio, whereas for the samples preincubated with DMPC the activity remains approximately constant at $\sim$1400 min^{-1} mg^{-1} which is comparable with the activity of the enzyme as isolated (typically 1500 min^{-1} mg^{-1}).

The ESR spectra of the 14-PCSL spin-label in DMPC-substituted complexes of various lipid/protein ratios are given in Figure 2. The sample temperature was 32 °C which is above the ordered-fluid bilayer phase transition of all the different complexes. All of the spectra consist of two easily differentiated components: a component which is strongly immobilized on the spin-label ESR time scale in addition to the component which corresponds more closely to the fluid lipid bilayer. The proportion of the immobilized component increases systematically with increasing protein content of the complexes and arises from a specific immobilization of the lipid by the protein, since it is not present in bilayers of the pure lipid (bottom spectrum of Figure 2). Figure 3 gives the fluid-component difference spectra obtained by subtracting the same immobilized component from the spectra of each of the different lipid/protein ratio complexes in Figure 2. The immobilized spectrum was obtained from an extensively delipidated sample of cytochrome oxidase, at a somewhat higher temperature (36 °C) and with a slight correction made in the splitting for the different polarity of the environment (Smith et al., 1976; Griffith et al., 1974). The difference spectra of Figure 3 are all characteristic of the 14-PCSL label in a relatively fluid bilayer environment, although with some systematic change in the degree of mobility with lipid/protein ratio.

The relative proportions of the immobilized and fluid components were obtained by double integration of the component spectra and are given in Figure 4. Since the total lipid/protein ratio, n_t, is simply the sum of the immobilized and fluid components, $n_t = n_f + n_b$, where n_b (n_f) is the number of immobilized (fluid) lipids per protein, the lipid/protein titration can be expressed as

$$n_f/n_b = n_t/n_b - 1 \qquad (1)$$

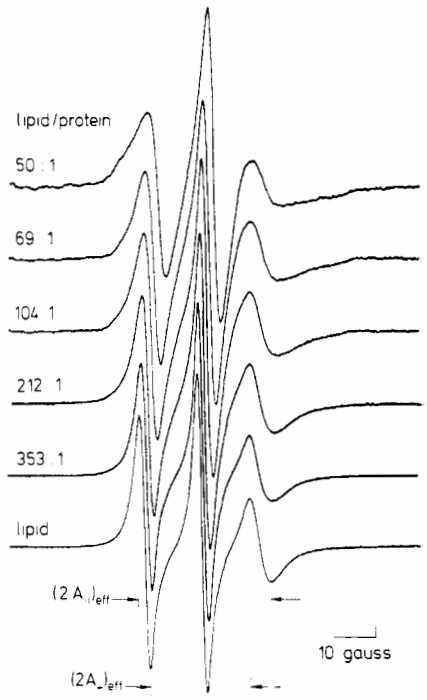

FIGURE 3: ESR difference spectra of the fluid lipid bilayer component obtained by subtracting the immobilized component from the spectra of the complexes in Figure 2.

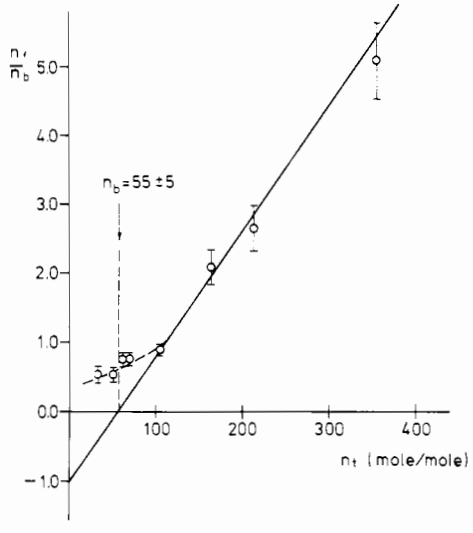

FIGURE 4: Lipid–protein titration of cytochrome oxidase–DMPC complexes from the spin-label difference spectra of Figure 3. n_b is the immobilized part of the total lipid/protein ratio, n_t, which must be subtracted from the spectra of the complexes to yield the fluid component, n_f.

Thus, the linear region of Figure 4, with the intercept of −1 on the n_f/n_b axis, indicates that at the higher lipid/protein ratios a constant number, $n_b = 55 \pm 5$, of immobilized lipid molecules is associated with each protein, independent of the total amount of lipid in the complex. In this sense the immobilized component can be defined as the first shell of lipid associated with the protein. Departures from linearity are observed in Figure 4 at low lipid/protein ratios (<100:1) at which the quantity of immobilized lipid exceeds that of the fluid lipid. This can possibly be interpreted in terms of the competitive binding of lipid to lipid vs. lipid to protein, which gives rise to a heterogenous sample with some lipid-rich regions and some partially aggregated protein.

The agreement of Figure 4 with the functional form of eq 1 also justifies the implicit assumption that the 14-PCSL label

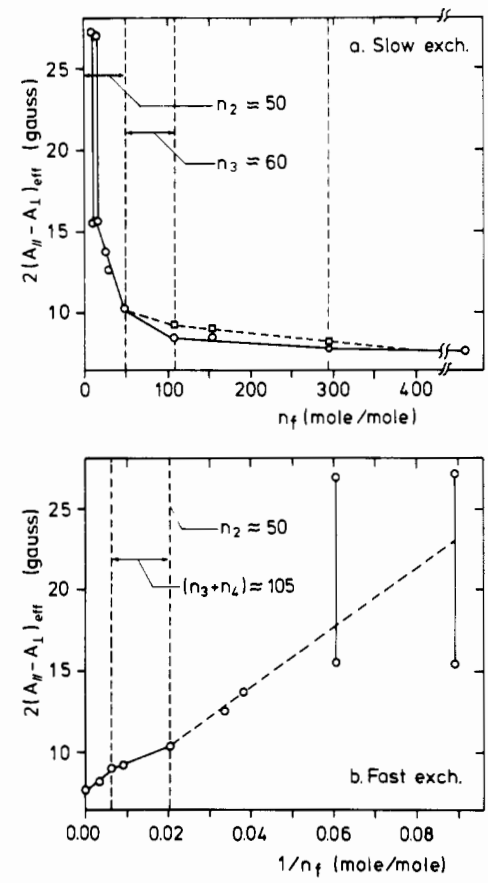

FIGURE 5: Variation of the empirical line width and splitting parameter $2(A_\parallel - A_\perp)_{eff}$ of the fluid lipid bilayer component spectra of Figure 3 as a function of the lipid/protein ratio. (a) Variation with n_f both without (--□--) and with (–O–) correction for the underlying shells by subtraction, assuming slow exchange. (b) Variation with $1/n_f$ assuming fast exchange between the extra-boundary shells.

reflects the distribution of the unlabeled PC in an exact 1:1 fashion. Alternatively, Griffith & Jost (1978) have modeled this system as an exchange equilibrium between labeled and unlabeled lipids occupying n_1 independent sites on the protein. Then

$$n_f/n_b = n_t/(n_1 K_r) - 1/K_r \qquad (2)$$

where K_r is the relative binding constant of labeled lipid compared with unlabeled lipid. Clearly, from Figure 4, $K_r = 1$, again implying no selectivity between labeled and unlabeled lipid.

The progressive changes in the fluid-component difference spectra of Figure 3 as a function of lipid/protein ratio have been characterized by the empirical parameter $(A_\parallel - A_\perp)_{eff}$ defined in Figure 3. This parameter is determined by both line splittings and line widths and thus is dependent on both the amplitude and rate of molecular motion, although in this spectral range it is difficult to distinguish between the two (Schreier et al., 1978). The changes in $(A_\parallel - A_\perp)_{eff}$ with lipid/protein ratio are given in Figure 5a (broken line) and represent the perturbation by the protein of the lipids beyond the first immobilized shell. Since it is not known whether the exchange of lipid molecules between these more distant shells is fast or slow on the spin-label time scale, the data have been analyzed under both conditions.

For slow exchange the spectra must be corrected for the contributions of the underlying shells by subtraction of these components. The total ESR signal is given by Sig $\sim (1/n_t)\sum_i n_i s_i$, where s_i is the contribution from the ith shell which contains n_i molecules. Since only the first (immobilized) shell

is resolved, it is assumed on geometric grounds that the numbers of molecules in the higher shells are given by $n_i = 55 + 8(i - 1)$. For two complexes with lipid/protein ratios n_t^I and n_t^{II} which extend to the Nth and $(N + 1)$th shells, respectively, Sig^{II} can be approximately corrected by subtraction of Sig^I to yield the spectrum of the $(N + 1)$th shell:[2]

$$s_{N+1} \propto Sig^{II} - (\sum_{i=1}^{N} n_i/n_t^{II})Sig^I \qquad (3)$$

where the sum extends to a filled Nth shell. The results of such subtractions yield reasonable spectral shapes for the single-shell components and thus are not inconsistent with slow exchange. The variation of the single-shell values of $(A_{||} - A_\perp)_{eff}$ with lipid/protein ratio is given in Figure 5a (solid line). From this it can be seen that the perturbations beyond the first (immobilized) shell fall into roughly three regions: a second shell of $n_2 \simeq 50$ molecules which is markedly perturbed, a third shell of $n_3 \simeq 60$ molecules which is less strongly perturbed, and the region $n_f \sim 110$ to $n_f \sim 300$ which accounts for ca. two to three further shells which are only weakly perturbed, if at all. Within the n_2 shell, complexes in which only the first half is filled ($n_f \leq 25$) are very strongly perturbed relative to those in which the second half of the shell is also filled. This strongly perturbed region probably corresponds to a single shared shell between two proteins (complete with their boundary layer) and thus is the combined effect of the overlap of the perturbation from both proteins. Such shared-shell effects are probably quite general and would lead to an apparently continuous rather than stepwise change between shells (cf. Figure 5a).

If the shells beyond the boundary layer are in fast exchange, the observed value of $\Delta = (A_{||} - A_\perp)_{eff}$ will be given by the weighted mean of the values, Δ_i, appropriate to the individual occupied shells, i.e., $\Delta \sim (1/n_f)\sum n_i\Delta_i$. For a complex for which n_f lies within the $(N + 1)$th shell

$$\Delta \simeq (\sum_{i=2}^{N} n_i\Delta_i - \Delta_{N+1}\sum_{i=2}^{N} n_i)(1/n_f) + \Delta_{N+1} \qquad (4)$$

Thus, in the case of the fast exchange, a plot of $\Delta = (A_{||} - A_\perp)_{eff}$ against $1/n_f$ should be linear within a given shell, with a change in gradient at the shell boundary only if the next higher shell has a different value of Δ_i. The primary data of Figure 5a (broken line) are plotted in this way in Figure 5b. The dependence on $1/n_f$ is consistent with fast exchange between a perturbed second shell of $n_2 \simeq 50$ molecules, two further less strongly perturbed shells of $n_3 + n_4 \simeq 105$ molecules, and the remainder of the lipid which is essentially unperturbed relative to protein-free bilayers. (Strong perturbations, corresponding to shared-shell effects as noted above, are observed for complexes lying within the n_2 shell. These have no further shells with which to exchange.) From Figure 5b, it is found that $\Delta_2 \sim 5.2$ G for a filled second shell, compared with $\Delta_\infty \sim 3.8$ G for pure lipid bilayers. Complete averaging by fast exchange, as indicated in Figure 5b, would therefore require an exchange rate of $>(\Delta_2 - \Delta_\infty)g\beta$, i.e., $>4.10^6$ s^{-1}, which is of the same order of magnitude as for lipid–lipid exchange in unperturbed bilayers. Thus, the data are consistent with either fast or slow exchange but cannot distinguish between them.

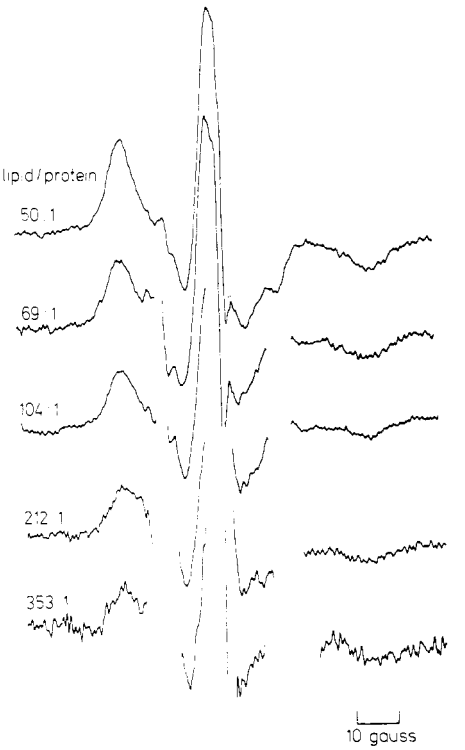

FIGURE 6: ESR difference spectra of the immobilized lipid component in cytochrome oxidase–DMPC complexes, obtained by subtracting the fluid lipid bilayer component from the spectra of Figure 2.

Table I: Variation of the Effective Rotational Correlation Times of the 14-PCSL Spin-Label in the Immobilized Regions of Cytochrome Oxidase–DMPC Complexes, as a Function of the Lipid/Protein Ratio, at 32 °C[a]

lipid/protein	τ_R (ns)[b]	τ_R (ns)[c]	τ_R (ns)[d]
353:1	25	75	32
212:1	21	79	34
162:1	30	83	47
104:1	29	83	51
69:1	22	65	39
61:1	38	493	32
50:1	29	144	49
32:1	31	>1000	46

[a] A_{zz}^R, ΔH_l^R, and ΔH_h^R were obtained from an extensively delipidated sample at 1 °C. [b] Deduced from the outer splitting, A_{zz}. [c] Deduced from the low-field line width, ΔH_l. [d] Deduced from the high-field line width, ΔH_h.

Difference spectra corresponding to the immobilized lipid component in the various complexes are given in Figure 6. The fluid component for these subtractions was obtained from sonicated DMPC vesicles at temperatures close to the phase-transition temperature. It was not possible to obtain an exact match in the center part of the spectrum because of the varying line shapes of the fluid component with the lipid/protein ratio (cf. Figures 3 and 5). However, sufficiently good resolution was obtained in the outer wings of the spectrum, which is the region most useful for analyzing slow motions of the spin-label (Freed, 1976). An estimate of the motional correlation time of the immobilized labels can be obtained from the line width of the high (low) field outermost peak, $\Delta H_{h(l)}$, or from the peak separation, $2A_{zz}$, if the corresponding values, $\Delta H_{h(l)}^R$ and A_{zz}^R, for completely, rigidly immobilized spin-labels are known. The empirical equations $\tau_R = a(1 - A_{zz}/A_{zz}^R)^b$ and $\tau_R = a_m'(\Delta H_m/\Delta H_m^R - 1)^{b_m'}$ are

[2] A more exact correction is given by the recurrence relation for the single-shell components:

$$s_{N+1} \propto (n_t^{II}Sig^{II} - n_t^{I}Sig^{I}) - (n_t^{II}/n_t^{I})(\sum_{i=1}^{N} n_i - n_t^{I})s_N$$

By choosing the complex I to have n_t^I lying closest to the filled Nth shell value, $\sum_i^N n_i$, the correction term involving s_N will be small and s_N may be approximated by the difference spectra obtained by previous application of this relation to Sig^I. The results obtained by this procedure are found to be not very different from those obtained from the more approximate relation (eq 3).

used, where the calibration constants are obtained by simulation: $a_h' = 2.12 \times 10^{-8}$ s, $b_h' = -0.778$, $a_l' = 1.15 \times 10^{-8}$ s, $b_l' = -0.943$, $a = 5.4 \times 10^{-10}$ s, $b = -1.36$ (Freed, 1976). For anisotropic motion this gives the correlation time for the motion of the nitroxide z axis. The absolute values of the correlation times are critically dependent on the choice of the appropriate rigidly immobilized spectrum, but changes in correlation time should be less so. Table I gives the variation in effective correlation time with lipid/protein ratio, taking the spectrum of an extensively lipid-depleted sample of cytochrome oxidase at 1 °C for the rigid limit parameters. The effective correlation times measured by a given parameter all give approximately the same value independent of lipid/protein ratio, implying that the motion of the immobilized component is dominated by the protein rather than by the lipid. The τ_R values obtained from A_{zz} are consistently lower because of the higher polarity of the depleted samples, which increases A_{zz} for nonmotional reasons. Since the immobilized component is reasonably approximated by the spectrum of an extensively lipid-depleted sample at 36 °C, it is possible that the values in Table I are a lower limit. This would imply that $\tau_R \gtrsim 50$ ns for the first shell immobilized lipid, i.e., motion at least 50 times slower than in the fluid state.

Discussion

The spin-label results indicate the coexistence of a population of immobilized lipid and a population of fluid lipid at all lipid/protein ratios studied. It is unlikely that these two populations correspond to physically different lipid–protein complexes, since the preparation method gives essentially homogeneous samples on density gradient analysis and the fluid components themselves show systematic spectral changes with lipid/protein ratio (Figure 3). At lipid/protein ratios for which the fluid population is of the same size or greater than the immobilized population, a constant number of lipids per protein are immobilized, irrespective of the total amount of lipid present. This suggests that the lipid is immobilized by direct interaction with the hydrophobic surface of isolated protein monomer or oligomer units rather than by being trapped between the protein units as a result of high packing density [cf. Marsh et al. (1978)]. Jost et al. (1973a) attributed a similar immobilized lipid population in beef heart cytochrome oxidase to a first shell or boundary layer around the protein, since it was calculated from electron microscopy that approximately 50 lipids could be accommodated around the protein. Frey et al. (1978) have recently performed negative-stain electron microscopy on lattice preparations of the yeast enzyme and found lattice dimensions similar to those for the beef heart enzyme. Thus, the present value of $n_b = 55 \pm 5$ would also be consistent with a single boundary layer of immobilized lipid for the yeast enzyme. However, the value of 50 molecules/protein surface may be an underestimate since electron microscopy studies at higher resolution (Henderson et al., 1977) suggest that the perimeter of the protein may be extensively invaginated. If this is the case, the immobilized component might be solely the lipid which is accommodated within the surface invaginations of the protein.

The ESR results on the fluid component indicate that the influence of the protein on the lipid fluidity extends beyond the first boundary layer shell. At least two further shells are perturbed and possibly up to three further shells are weakly perturbed, depending on whether the shells are in fast exchange. At low lipid/protein ratios ($n_f < 25$) the lipid outside the boundary layer is strongly perturbed as a result of being shared or "trapped" (Marsh et al., 1978) between adjacent proteins. Since this extra restriction of motion, which is quite different from the strong immobilization of the boundary layer, arises from overlapping lipid shells, it could provide a means of communication between neighboring proteins.

The dependence of the specific activity of the enzyme on the lipid/protein ratio (Figure 1a) parallels the classification of the lipid shells deduced from the spin-label immobilization data (cf. Figure 1b). As the lipid content is reduced below the boundary ratio ($n_t \leq 50$), the activity decreases sharply. It thus appears that the first boundary shell of lipid is required to keep the enzyme in potentially active form. At lipid/protein ratios greater than the first-shell value, the activity is still less than that maximally regenerable but increases steadily to this value with increasing lipid content. This may be due to the effect of the subsequent shells of lipid (cf. Figure 1b). Alternatively, it is possible that DMPC alone does not as readily support full activity as does asolectin, for example, or detergents such as Tween 80 (Yu et al., 1975; Robinson & Capaldi, 1977; Vik & Capaldi, 1977). High activity was only obtained after preincubation of the complexes with cholate. However, this cholate should be almost completely diluted away in the assay mixture (Warren et al., 1974a), and cholate itself does not support high activity (Yu et al., 1975; Robinson & Capaldi, 1977; Virji & Knowles, 1978). The cholate may therefore simply ensure access of substrate to the enzyme as explained previously, but a synergistic action with the lipid cannot be excluded.

The spin-label characterization of the immobilization of the various lipid shells requires further clarification. It is not possible to determine from the spectra of Figure 6 (or of Figure 3) whether the observed immobilization is accompanied by a change in degree of order (or angular amplitude of motion) of the lipid chains. Since the immobilized component (Figure 6) corresponds to motion which is slow on the conventional ESR time scale, it occupies the full spectral anisotropy of the nitroxide group independent of the amplitude of motion. However, ESR experiments with oriented cytochrome oxidase preparations (Jost et al., 1973b) suggest that the immobilized lipid might be completely disordered, and deuterium NMR experiments (Seelig & Seelig, 1978) also have been interpreted in terms of a lipid population around the protein which has lower order but is in fast exchange with the lipid of the bilayer. The fluid components (Figure 3) are in a spectral regime in which it is very difficult to distinguish between changes in rate of motion and changes in order (Schreier et al., 1978). A previous quantitation of the restriction of motion was made in terms of an order parameter (Marsh et al., 1978), which for these spectra does not distinguish between different rates and amplitudes of motion. Thus, the net mobility decrease in Figure 4 represents the combined result of these two effects.

Regarding the rate of exchange between the various lipid shells, the boundary layer, or first shell, is in slow exchange with the other shells since separate spectra are resolved. The data for the subsequent shells cannot distinguish between fast and slow exchange, but an intershell exchange rate of $>8 \times 10^6$ s^{-1} would be required for fast exchange. An upper limit for the exchange rate of the first-shell lipid is given by the correlation times of Table I, i.e., $\tau_{ex} > 50$ ns. However, it is more likely that Table I refers to τ_k, the rotational correlation time for segmental motion of the lipid chains. The molecular model proposed by Galla & Sackmann (1974) for lipid lateral diffusion can then be used to estimate the exchange rate in terms of τ_k. In the model, the rate of lateral displacement, ν_l, is determined by the concentration of rotational isomers, c_k, and the time taken to migrate along the length (l) of the chain: $\nu_l \sim (c_k \Delta_k^2/\tau_k)/l^2$, where $\Delta_k = 1.26$ Å is the projected

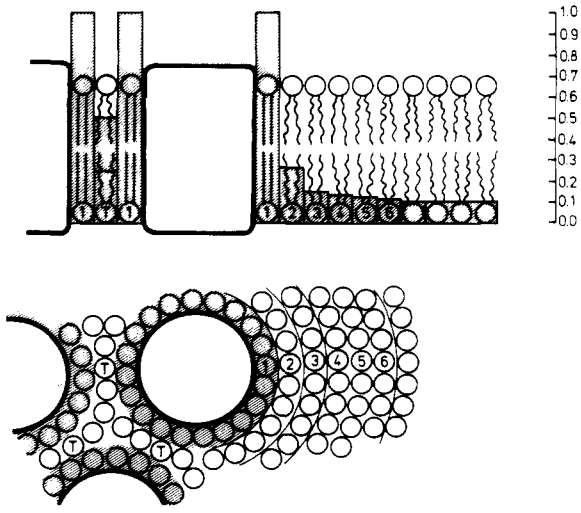

FIGURE 7: Schematic indication of the degree of chain immobilization in the various shells of lipid surrounding cytochrome oxidase in DMPC complexes. The vertical scale corresponds to values of $(A_{\parallel} - A_{\perp})_{eff}$ normalized with respect to the maximum hyperfine anisotropy of 25 G. Details beyond the second shell depend on whether the lipids are in fast or slow exchange. T is a shared second shell which exists only in regions of high protein packing density (low lipid/protein ratios) where the perturbations from two adjacent protein molecules overlap.

length of a C–C bond. Lipid chains next to the protein may be more disordered than in the bilayer; hence, c_k could be up to a factor of 4 greater for the first-shell lipids[3] than for the bilayer lipids whereas their immobilization increases τ_k by ~50 times relative to the bilayer lipids (Table I). Thus, the exchange between the immobilized and fluid lipid can be at least 10 times slower than the lipid–lipid exchange in unperturbed bilayers,[4] i.e., $\nu_{ex} < 10^5$–10^6 s^{-1}. This estimate is consistent with the finding that in a beef heart cytochrome oxidase–lipid system the boundary layer exchanges fast on the ^{2}H NMR time scale: $\nu_{ex} > 10^4$ s^{-1} (Seelig & Seelig, 1978). Since the turnover number for yeast cytochrome oxidase is ~300 s^{-1} (Mason et al., 1973), it is probable that the boundary layer is at equilibrium during the catalytic cycle. Thus, it is the conformation and mobility of the boundary lipid, as seen for instance by ESR, and not its exchange rate which are likely to affect the enzyme activity.

In summary (see Figure 7), the present studies have revealed at least three classes of lipid shells, other than unperturbed bilayer, which may arise in membranes as a result of lipid–protein interactions. The first is the boundary layer whose properties are largely dominated by the hydrophobic surface of the protein; the second is the trapped lipid or shared lipid shell whose existence is determined by the protein packing density and is only present in complexes with insufficient lipid to form a complete second shell around every protein; the third environment consists of the shells outside the boundary layer which form a continuous contact with the bilayer and whose perturbation falls off fairly steeply beyond the first extra-boundary shell. The rate of exchange between the shells is likely to be fast relative to the enzyme catalytic rates, and thus it is their dynamic structure, not the exchange rate, which is likely to determine the functional lipid–protein interaction. Recent theoretical studies (Owicki et al., 1978) have indicated that the nature of lipid–protein interactions is very strongly dependent on the way in which the lipid molecules match the hydrophobic span of the protein (i.e., the boundary conditions) and that the range of the interaction is extremely temperature dependent if in the region of a lipid phase transition. Thus, different lipid/protein systems could have very different lipid/protein interactions, and detailed generalizations are not possible. However, it is to be expected that some biological membranes will display the features of lipid–protein interactions described here. Indeed, a strongly immobilized lipid component has been observed in some natural membranes (Takeuchi et al., 1978; Marsh & Barrantes, 1978; Birrell et al., 1978; Watts et al., 1979), and the apparent differences in order parameters between some membranes and their lipid bilayers (Gaffney & Lin, 1975; Gaffney & Chen, 1977) may correspond to an unresolved immobilized component in addition to perturbations of the extra-boundary shells.

[3] The fraction of gauche rotational isomers per C–C bond is ~0.25 in fluid lipid bilayers (Marsh, 1974; Träuble & Haynes, 1971); hence, the maximum increase in gauche rotational isomers is by a factor of 4. In the model of Galla & Sackmann (1974), c_k refers specifically to kink rotational isomers of which there is ca. one per chain in fluid lipid bilayers. The maximum number is ca. four kinks per chain, again giving a maximum possible increase in c_k of a factor of 4.

[4] Two canceling factors of 2 are omitted in this estimate. First, of the two molecules involved in the exchange, only the boundary molecule is strongly perturbed, but, second, only approximately half the sites is available for exchange compared with a lipid molecule in an extended bilayer region.

Acknowledgments

We thank U. Bottin and R. Boyes for their expert technical assistance.

References

Birrell, G. B., Sistrom, W. R., & Griffith, O. H. (1978) *Biochemistry 17*, 3768.
Boss, W. F., Kelley, C. J., & Landsberger, F. R. (1975) *Anal. Biochem. 64*, 289.
Brown, M. F., Miljanich, G. P., & Dratz, E. A. (1977) *Biochemistry 16*, 2640.
Curatolo, W., Sakura, J. D., Small, D. M., & Shipley, G. G. (1977) *Biochemistry 16*, 2313.
Dulley, J. R., & Grieve, P. A. (1975) *Anal. Biochem. 64*, 136.
Eibl, H., & Lands, W. E. M. (1969) *Anal. Biochem. 30*, 51.
Eytan, G. D., & Schatz, G. (1975) *J. Biol. Chem. 250*, 767.
Freed, J. H. (1976) in *Spin Labelling* (Berliner, L. J., Ed.) Academic Press, New York.
Frey, T. G., Chan, S. H. P., & Schatz, G. (1978) *J. Biol. Chem. 253*, 4389.
Gaffney, B. J., & Lin, D. C. (1975) in *Membrane-Bound Enzymes* (Martonosi, A., Ed.) Vol. 1, Wiley, New York.
Gaffney, B. J., & Chen, S.-C. (1977) *Methods Membr. Biol. 8*, 291.
Galla, H.-J., & Sackmann, E. (1974) *Ber. Bunsenges. Phys. Chem. 78*, 949.
Griffith, O. H., & Jost, P. C. (1978) in *Proceedings of the Japanese-American Seminar on Cytochrome Oxidase* (Chance, B., King, T. E., Okunuki, K., & Orii, Y., Eds.) Elsevier, Amsterdam.
Griffith, O. H., Dehlinger, P. J., & Van, S. P. (1974) *J. Membr. Biol. 15*, 159.
Henderson, R., Capaldi, R. A., & Leigh, J. S. (1977) *J. Mol. Biol. 112*, 631.
Hubbell, W. L., & McConnell, H. M. (1971) *J. Am. Chem. Soc. 93*, 314.
Jost, P. C., Griffith, O. H., Capaldi, R. A., & Vanderkooi, G. (1973a) *Proc. Natl. Acad. Sci. U.S.A. 70*, 480.
Jost, P. C., Griffith, O. H., Capaldi, R. A., & Vanderkooi, G. (1973b) *Biochim. Biophys. Acta 311*, 141.
Marčelja, S. (1976) *Biochim. Biophys. Acta 455*, 1.
Marsh, D. (1974) *J. Membr. Biol. 18*, 145.
Marsh, D., & Barrantes, F. J. (1978) *Proc. Natl. Acad. Sci. U.S.A. 75*, 4329.

Marsh, D., Watts, A., Maschke, W., & Knowles, P. F. (1978) *Biochem. Biophys. Res. Commun. 81*, 397.
Mason, T. L., Poyton, R. O., Wharton, D. C., & Schatz, G. (1973) *J. Biol. Chem. 248*, 1346.
Owicki, J. C., Springgate, M. W., & McConnell, H. M. (1978) *Proc. Natl. Acad. Sci. U.S.A. 75*, 1616.
Robinson, N. C., & Capaldi, R. A. (1977) *Biochemistry 16*, 375.
Scandella, C. J., Devaux, P., & McConnell, H. M. (1972) *Proc. Natl. Acad. Sci. U.S.A. 69*, 2056.
Schreier, S., Polnaszek, C. F., & Smith, I. C. P. (1978) *Biochim. Biophys. Acta 515*, 375.
Seelig, A., & Seelig, J. (1978) *Hoppe-Seyler's Z. Physiol. Chem. 359*, 1747.
Smith, I. C. P., Schreier-Muccillo, S., & Marsh, D. (1976) in *Free Radicals in Biology* (Pryor, W. A., Ed.) Vol. 1, Academic Press, New York.
Smith, L. (1955) *Methods Biochem. Anal. 2*, 427–434.
Stoffel, W., Zierenberg, O., & Scheefers, H. (1977) *Hoppe-Seyler's Z. Physiol. Chem. 358*, 865.
Takeuchi, Y., Ohnishi, S.-I., Ishinaga, M., & Kito, M. (1978) *Biochim. Biophys. Acta 506*, 54.
Träuble, H., & Haynes, D. H. (1971) *J. Membr. Biol. 7*, 324.
Träuble, H., & Sackmann, E. (1972) *J. Am. Chem. Soc. 94*, 4499.
Vaz, W. L. C., Vogel, H., Jähnig, F., Austin, R. H., & Schoellmann, G. (1978) *FEBS Lett. 87*, 269.
Vik, S. B., & Capaldi, R. A. (1977) *Biochemistry 16*, 5755.
Virji, M., & Knowles, P. F. (1978) *Biochem. J. 169*, 343.
Warren, G. B., Toon, P. A., Birdsall, N. J. M., Lee, A. G., & Metcalfe, J. C. (1974a) *Biochemistry 13*, 5501.
Warren, G. B., Toon, P. A., Birdsall, N. J. M., Lee, A. G., & Metcalfe, J. C. (1974b) *Proc. Natl. Acad. Sci. U.S.A. 71*, 622.
Watts, A., Marsh, D., & Knowles, P. F. (1978) *Biochem. Biophys. Res. Commun. 81*, 403.
Watts, A., Volotovski, I. D., & Marsh, D. (1979) *Biochemistry* (in press).
Yonetani, T., & Ray, G. S. (1965) *J. Biol. Chem. 240*, 3392.
Yu, C., Yu, L., & King, T. E. (1975) *J. Biol. Chem. 250*, 1383.

Phosphorus-31 Nuclear Magnetic Resonance Studies of Wild-Type and Glycolytic Pathway Mutants of *Saccharomyces cerevisiae*†

Gil Navon,‡ Robert G. Shulman,* Tetsuo Yamane, T. Ross Eccleshall,* Keng-Bon Lam,§ Jerald J. Baronofsky, and Julius Marmur

ABSTRACT: High-resolution phosphorus-31 nuclear magnetic resonance (^{31}P NMR) spectra of wild-type and mutant strains of *Saccharomyces cerevisiae* were observed at a frequency of 145.7 MHz. Levels of various phosphorus metabolites were investigated upon addition of glucose under both aerobic and anaerobic conditions. Three mutant strains were isolated and their biochemical defects characterized: *pfk* lacked phosphofructokinase activity; *pgi* lacked phosphoglucose isomerase activity; and *cif* had no glucose catabolite repression of the fructose bisphosphatase activity. Each mutant strain was found to accumulate characteristic sugar phosphates when glucose was added to the cell suspension. In the case of the phosphofructokinase deficient mutant, the appearance of a pentose shunt metabolite was observed. ^{31}P NMR peak assignments were made by a pH titration of the acid extract of the cells. Separate signals for terminal, penultimate, and central phosphorus atoms in intracellular polyphosphates allowed the estimation of their average molecular weight. Signals for glycero(3)phosphocholine, glycero(3)phosphoserine, and glycero(3)phosphoethanolamine as well as three types of nucleotide diphosphate sugars could be observed. The intracellular pH in resting and anaerobic cells was in the range 6.5–6.8 and the level of adenosine 5′-triphosphate (ATP) low. Upon introduction of oxygen, the ATP level increased considerably and the intracellular pH reached a value of pH 7.2–7.3, irrespective of the external medium pH, indicating active proton transport in these cells. A new peak representing the inorganic phosphate of one of the cellular organelles, whose pH differed from the cytoplasmic pH, could be detected under appropriate conditions.

Previous studies have shown the usefulness of high-resolution ^{31}P NMR[1] in monitoring intracellular concentrations of phosphate metabolites in suspensions of whole cells from mammalian (Moon & Richards, 1973; Henderson et al., 1974; Navon et al., 1977a, 1978; Evans & Kaplan, 1977) and microbial (Salhany et al., 1975; Navon et al., 1977b; Ugurbil et al., 1978) origins.

On the basis of chemical shifts of inorganic phosphate and other phosphate metabolites, the intracellular pH can be determined (Moon & Richards, 1973; Salhany et al., 1975; Navon et al., 1977a,b). In a previous study on endogenous

† From Bell Laboratories, Murray Hill, New Jersey 07974 (G.N., R.G.S., and T.Y.), and the Department of Biochemistry, Albert Einstein College of Medicine, Bronx, New York 10461 (T.R.E., K-B.L., J.J.B., and J.M.). *Received February 28, 1979.* Partial support for T.R.E. was from 1T32 AG 00052-01. Support for J.J.B. was from 5T32 GM 07128. Partial support for J.M. was obtained from 2P50 GM 19100. The part of this work done at Einstein was partially supported by 5R01 CA 12410.

‡ Permanent address: Department of Chemistry, Tel Aviv University, Ramat Aviv, Tel Aviv, Israel.
§ Present address: Connaught Laboratories, Ltd., Willowdale, Ontario, Canada M2N 5T8.

[1] Abbreviations used: DHAP, 1,3-dihydroxyacetone phosphate; FBP, fructose 1,6-bis(phosphate); F6P, fructose 6-phosphate; GAP, glyceraldehyde 3-phosphate; GPC, glycero(3)phosphocholine; GPE, glycero(3)phosphoethanolamine; GPS, glycero(3)phosphoserine; G6P, glucose 6-phosphate; NADH, β-nicotinamide adenine dinucleotide (reduced form); NADPH, β-nicotinamide adenine dinucleotide phosphate (reduced form); NAD^+, β-nicotinamide adenine dinucleotide (oxidized form); NMR, nuclear magnetic resonance; PEP, phosphoenolpyruvate; 3PGA, 3-phosphoglycerate; 6PGA, 6-phosphogluconate; P_i, inorganic phosphate; UDPG, uridinediphosphoglucose; YP, 1% Difco yeast extract + 2% Difco peptone; YPD, YP + 2% glucose; YPF, YP + 2% fructose; YPFGal, YP + 2% fructose + 2% galactose; YPGE, YP + 3% glycerol + 2% ethanol. Enzyme Commission numbers: phosphoglucoisomerase, 5.3.1.9; phosphofructokinase, 2.7.1.11; and fructose bisphosphatase, 3.1.3.11.

0006-2960/79/0418-4487$01.00/0